Biochemistry and Biophysics Reports 38 (2024) 101726

Contents lists available at ScienceDirect

Biochemistry and Biophysics Reports

journal homepage: www.elsevier.com/locate/bbrep

Resistive spontaneous breathing exacerbated lipopolysaccharide-induced lung injury in mice

Zhigui Cai, Huanhuan Zhang [1], Xingxing Guo, Liqiang Song [*]

Department of Pulmonary and Critical Care Medicine, Xijing Hospital, Air Force Medical University, Xi'an, China

ARTICLE INFO

Keywords:
ARDS
Resistive spontaneous breathing
Lung injury
P-SILI
Piezo1

ABSTRACT

Background: Spontaneous respiratory mechanical force interacted with the primary lung injury and aggravated the progression of ARDS clinically. But the exact role and involved mechanism of it in the pathogenesis of ARDS animal model remained obscure.

Aim: This study was to investigate the effect of spontaneous respiratory mechanical force on lung injury of ARDS in mice.

Methods: Female C57BL/6 mice were subjected to resistive spontaneous breathing (RSB) by tracheal banding after 4–6 h of intranasal inhalation of LPS. Pulmonary function was examined by Buxco system, partial pressures of oxygen and carbon dioxide (PO_2 and PCO_2) were measured by a blood gas analyzer, and lung pathological changes were analyzed with hematoxylin and eosin staining. The levels of inflammatory markers were quantified by ELISA, total protein assay, and FACS analysis. The expression levels of mechanosensitive ion channels were detected by qRT-PCR and immunohistochemistry.

Results: The airway resistance (Raw) was increased and the tidal volume (TV) was decreased remarkedly in RSB group. RSB treatment did not affect PO_2, PCO_2, pathology and inflammation levels of lung in mice. The Raw increased and ventilatory indicators decreased in RSB + ARDS compared to ARDS significantly. Besides, RSB treatment deteriorated the changes of PO_2, PCO_2 and level of lactic acid induced by LPS. Meanwhile, RSB significantly promoted LPS-induced pulmonary histopathological injury, and elevated the levels of IL-1β, IL-6, TNF-α and total proteins, increased neutrophils infiltration. The expression level of Piezo1 in RSB + ARDS group was remarkably reduced compared to ARDS group and consistent with the severity of pulmonary damage.

Conclusion: RSB exacerbated LPS-induced ARDS hypoxemia and hypercapnia, inflammation and damage. The mechanosensitive protein Piezo1 expression decreased and may play an important role in the process.

1. Introduction

Acute respiratory distress syndrome (ARDS) is a clinical syndrome characterized by diffuse lung inflammation and non-cardiogenic pulmonary edema. The edema can have either pulmonary or systemic origin and commonly causes acute respiratory failure [1]. ARDS was identified in 10.4 % of patients admitted to intensive care units, with a mortality of as high as 34.9%–46.1 % in 2016 [1,2]. Due to the heterogeneity of ARDS, in-depth mechanistic studies and new treatments are needed.

Patients with severe lung injury usually have a high respiratory drive, which results in pulmonary regional forces and increased transmural pulmonary vascular pressure [3]. Experts defined lung injury caused by spontaneous high respiratory drive in non-intubated patients with acute respiratory failure as patient self-inflicted lung injury (P-SILI). P-SILI is typical lung injury exacerbated by spontaneous respiratory mechanical force. In addition, inspiratory resistive breathing leads to large negative swings in intrathoracic pressures and mechanical stress of structural cells of the lung [4] in many diseases, such as upper airway obstruction, chronic obstructive pulmonary disease (COPD) exacerbations, and asthma attacks [4]. Therefore, vigorous or feeble spontaneous breathing may induce lung damage in ARDS by exerting mechanical force on regional parenchyma. Theodoros and colleagues [5–7] showed that resistive breathing can change ventilation and pressure indices of pulmonary function in animal models. Toumpanakis and colleagues confirmed resistive breathing increased inhalational

* Corresponding author. Xijing Hospital, Air Force Medical University, No. 169, Changle West Road, Xi'an, Shaanxi, 710032, China.
E-mail address: songlq@fmmu.edu.cn (L. Song).
[1] The author contributed to the work equally and should be regarded as co-first author.

https://doi.org/10.1016/j.bbrep.2024.101726
Received 8 January 2024; Received in revised form 25 April 2024; Accepted 28 April 2024

LPS-induced lung injury score [8]. However, the effect of spontaneous respiratory mechanical force on ARDS animal model needs more comprehensive assessment.

Mechanosensitive ion channels (MSCs) play a crucial role in responding to mechanical forces and mediating the mechanosensation/mechanotransduction process [9]. MSCs, including epithelial sodium channel (ENaC), Piezo channels, transient receptor potential channels (TRPs), and two-pore domain potassium ion (K2P) channels, are not exclusively modulated by mechanical forces but are also affected by pH or inflammatory cytokines stimuli that are altered in ALI/ARDS lungs [10]. Specially, Piezo1 promoted the development and progression of ventilator-induced lung injury (VILI) by RhoA/ROCK1 signaling [11], which implied Piezo1 may participate in the spontaneous respiratory mechanical force aggravating the progression of ARDS. Here, this study investigated the effect of spontaneous respiratory mechanical force on hypoxemia, histopathology and inflammation in ARDS mouse model, and explored the potential mechanism by analyzing the changes of MSCs.

2. Materials and methods

2.1. Animals

Female C57BL/6J mice (8–10 weeks old, 20–25 g) were purchased from the Animal Center of Air Force Medical University. Mice were kept in air-filtered rooms, and have unrestricted access to semi-purified mouse food and pre-prepared water for drinking. Animals were housed at a constant temperature (20–24 °C) and constant humidity (50%–70 %) with a 12/12 h light/dark cycle. Animal experiments were conducted following the Guidelines for the Care and Use of Animals established by the Chinese government. The study protocol (IACUC-2023102) was approved by the Animal Care and Use Committee of Air Force Medical University.

2.2. Experimental models

2.2.1. RSB model

The animal model of RSB was induced through tracheal banding, as previously described [5,6]. Briefly, mice were anesthetized with an intraperitoneal injection of ketamine (90 mg/kg) and xylazine (5 mg/kg) and placed under a surgical microscope. The trachea was exposed, and a nylon band of a pre-specified length was introduced to below trachea and sutured around it to reduce its surface area [6]. Following recovery from anesthesia, mice were randomly assigned into 3 RSB groups. RSB was applied for 1 day, 3 days, and 5 days. Sham-operated animals were used for comparisons (controls). There were 10 mice in each group.

2.2.2. LPS-induced ARDS model

Khadangi and coworkers have shown that these two routes of administration are equivalent [12]. Mice were anesthetized by inhalation of isoflurane through an animal gas anesthesia machine. Then, mice were subjected to intranasal inhalation of LPS (5 mg/kg, in 50 μL saline) (Sigma-Aldrich, catalog no. L2880) [13].

2.2.3. RSB & ARDS joint model

The above two models were both used to simulate ARDS and concomitant RSB. Mice were subjected to the RSB model after 4–6 h of intranasal inhalation of LPS. RSB was applied for 3 days.

2.3. Pulmonary function test

Pulmonary function was assessed using the non-invasive Buxco NAM system (Connecticut, CT, USA) according to the manufacturer's instructions [14,15]. Briefly, mice were pre-adapted in the detecting room. Then mice were inserted within the restrainer and adjusted position by moving the locking mechanism to make sure that the mice's nares were protruding outside of the nose-cone with snouts resting against the inner walls of the restrainer. The restrainer containing the mouse was inserted through the rubber opening in the thoracic chamber and the mouse was allowed to relax for 5 min before recording of the nasal and thoracic flow signals. Respiratory parameters were monitored using the FinePointe software.

2.4. Arterial blood gas analysis

Arterial blood samples were collected from the left ventricle of mice using a heparinized syringe. Partial oxygen pressure (PaO_2), partial carbon dioxide pressure ($PaCO_2$), and blood lactic acid (Lac) level were analyzed using an ABL80Flex blood gas analyzer (Radiometer, Denmark).

2.5. Preparation of bronchoalveolar lavage fluid (BALF)

BALF was got in all mice as previous described [16]. In each mouse, 90 % (2.7 mL) of the total injection volume was continuously recovered. Following centrifugation of BALF at a speed of 520 g for a duration of 20 min at a temperature of 4 °C, the resulting liquid was reserved for future assessments.

2.6. Lung histopathology, inflammation score and immunohistochemistry (IHC)

The left lung was fixed with 5 % paraformaldehyde for 48 h, dehydrated by alcohol, embedded with paraffin wax, sliced into 4 μM sections, and stained with hematoxylin & eosin (H&E). After H&E staining, the pathological changes in lung tissue were observed under a conventional optical microscope. Ten nonoverlapping images per mouse were photographed and scored by a pulmonary pathologist in a blinded manner. The semiquantitative pathological changes of alveolar septal thickening, edema, inflammation, and hemorrhage were evaluated on a 1–4 scale (0, none; 1, mild; 2, moderate; 3, marked; 4, severe) [17,18].

Immunohistochemical staining for Piezo1 was performed using Piezo1 polyclonal antibody (Proteintech, catalog no. 15939-1-AP). The sections were de-paraffinized and sequentially treated for antigen epitope retrieval and endogenous peroxidase blocking. The sections were incubated with primary antibodies (1:200 dilution) overnight. After 5 min of incubation with DAB chromogen solution, the sections were counterstained with Mayer hematoxylin and dehydrated. As observed under the microscope, the degree of brown stains reflected the expression levels of Piezo1 in lung tissues.

2.7. Total protein assay

Total protein concentration in bronchoalveolar lavage fluid of mice was assessed using a BCA protein assay kit (Proteintech, catalog no. PK10026). The assay was conducted following the manufacturer's instructions.

2.8. Enzyme-linked immunosorbent assay (ELISA)

The concentrations of inflammatory factors IL-1β, TNF-α, and IL-6 in bronchoalveolar lavage fluid of mice were assessed using ELISA kits (Proteintech, catalog no. KE10003, KE10002, KE10007). The assay was conducted following the manufacturer's instructions.

2.9. Quantitative real-time PCR (qRT-PCR)

The total RNA of lung tissues was extracted using Trizol reagent (Thermo Fisher Scientific, catalog no. 15596018) following the manufacturer's protocols. cDNA was synthesized from 1 μg total RNA using PrimeScript RT Master Mix (TaKaRa, catalog no. RR036A). qRT-PCR

was performed using TB Green Premix Ex Taq II (TaKaRa, catalog no. RR820A) and CFX96 Touch Real-Time PCR Detection System (BioRAD). The primers used for the qRT-PCR were obtained from the PrimerBank website, as follows:

Piezo1-F 5′-CCTgTTACgCTTCAATgCTCT-3′
Piezo1-R 5′-gTgTAggCATATCTgAAAggCAA-3′
Aqp1-F 5′-AGGCTTCAATTACCCACTGGA-3′
Aqp1-R 5′-GTGAGCACCGCTGATGTGA-3′
Trek-1-F 5′-CCGAGGCTCTCATTCTCCTCA-3′
Trek-1-R 5′-AGGACGACCACCAGGAAAATC-3′
Scnn1a(ENaCα)-F 5′-CTGCTGGCTACTCAAGATGGC-3′
Scnn1a(ENaCα)-R 5′-AGGAGGCTGACCATCGTGAC-3′
Cdh23-F 5′-GCATCACTCAGAACACACCAG-3′
Cdh23-R 5′- CCTGCGTGACCTCATAGTCT-3′
Cdh1-F 5′-CTCCAGTCATAGGGAGCTGTC-3′
Cdh1-R 5′-TCTTCTGAGACCTGGGTACAC-3′
Gapdh-F 5′-TGTGTCCGTCGTGGATCTGA-3′
Gapdh-R 5′-TTGCTGTTGAAGTCGCAGGAG-3′

2.10. Flow cytometry

Mice were euthanized, and their lung tissues were collected. Single-cell suspensions were collected and stained with antibodies for fluorescence-activated cell sorting (FACS). Antibodies used for FACS were as follows: CD45-FITC (BioLegend, catalog no. 157214), Siglec F-PE (BioLegend, catalog no. 155505), Ly6G-APC (BioLegend, catalog no. 127614), CD11b-Pacific Blue (BioLegend, catalog no. 101223), and CD11c-BV421 (BD Biosciences, catalog no. 565452). The dilution of all antibodies was 1:200. Cells were sorted on a spectral cell analyzer (Sony, SA3800), and data were analyzed in FlowJo 10.9.0. Gating strategy

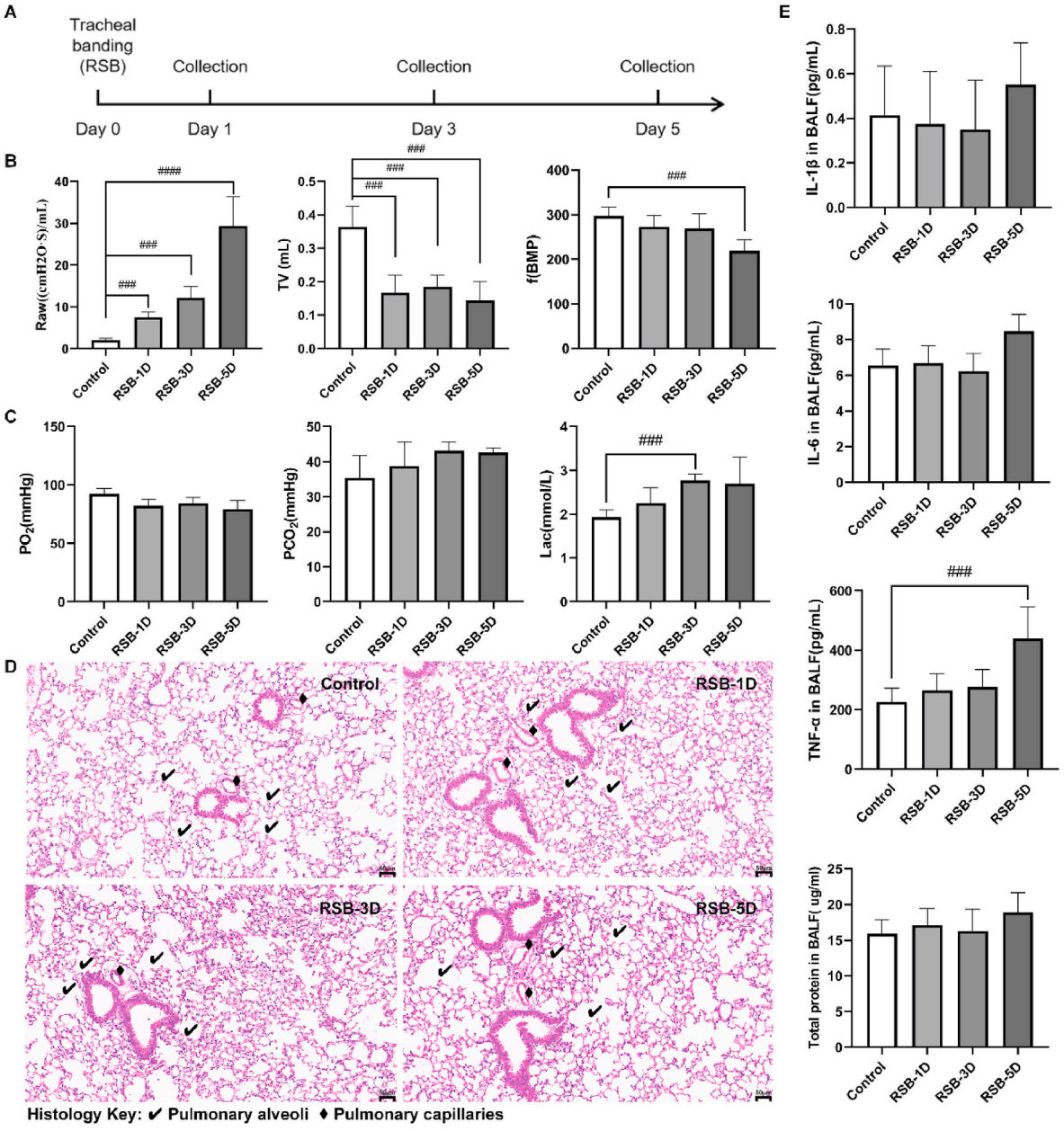

Fig. 1. RSB showed no significant lung injury in normal mice. 1d, 3d, and 5d after tracheal banding, (**A**) timeline of animal experimental protocol, (**B**) airway resistance (Raw), tidal volume (TV), the frequency (f), (**C**) partial pressure of oxygen (PO_2), partial pressure of carbon dioxide (PCO_2), blood level of lactic acid (Lac), (**D**) lung histopathological changes (200x magnification), (**E**) levels of IL-1β, IL-6, TNF-α and total proteins in bronchoalveolar lavage fluid (BALF) were analyzed. The values are indicated as mean ± SD (n = 8~10). $^{###}P < 0.001$, $^{####}P < 0.0001$, compared with the control group.

information can be found in Fig. s3.

2.11. Statistical analysis

All analyses were conducted using SPSS 23 for Windows (SPSS Inc, IBM). All data are presented as mean ± standard deviation. Differences between the control group and experimental groups were assessed using the one-way ANOVA method. P-values less than 0.05 were considered statistically significant.

3. Results

3.1. RSB in normal mice did not significantly cause lung injury

Pulmonary function, indices of arterial blood, and lung histopathology were measured to assess the effect of RSB on normal mice. Enhanced airway resistance and low tidal volume are the typical features of resistive breathing [4–7]. Compared with the control group, a reduction in tracheal surface area markedly increased airway resistance (Raw) ($P < 0.05$) and decreased tidal volume (TV), peak expiratory flow (PEF), and peak inspiratory flow (PIF) ($P < 0.05$), but did not significantly change respiratory rate (f), at least until day 3 (Fig. 1B and Fig. s1A). These findings indicate that spontaneous respiratory restriction was successfully induced. However, arterial blood gas analysis demonstrated that PO_2, PCO_2, and Lac did not significantly change after 1, 3, and 5 days of RSB, except for a significant increase in Lac on day 3 ($P < 0.05$). The results suggested no obvious acidosis or alkalosis, except for the indicative of mild acidosis on day 3. (Fig. 1C and Fig. s1B). Meanwhile, the integrity of pulmonary alveoli and capillaries was maintained and similar to that of the control group after RSB (Fig. 1D). IL-1β, IL-6, TNF-α, and total protein levels in the BALF of RSB were similar to those of the control group (Fig. 1E), except for TNF-α that was upregulated after 5 days of RSB ($P < 0.05$). The results of arterial blood gas analysis and lung histopathology suggested that RSB did not cause lung injury in normal mice.

3.2. RSB worsened LPS-induced respiratory dysfunction

The pulmonary function was the primary indicator of the effect of RSB on ARDS. The Raw of ARDS mice did not significantly change compared with control mice (Fig. 2B) [19]. However, a reduction in tracheal surface markedly increased the airway resistance of ARDS mice ($P < 0.05$). It revealed Raw may be a critical point of RSB's impact on ARDS. Furthermore, compared with the control group, the ARDS group exhibited a significant decrease in TV, minute volume (MV), PEF, PIF, and expiratory flow at 50 % of TV (EF50) ($P < 0.05$), and a significant increase in f ($P < 0.05$), but there was no significant difference in delta time (dT) (Fig. 2C–I). After adding RSB to LPS inhalation, all the above-mentioned indicators were significantly decreased ($P < 0.05$), except for a significant increase in dT ($P < 0.05$). These results suggested that spontaneous respiratory restriction intensified the respiratory dysfunction of ARDS mice.

3.3. RSB deteriorated LPS-induced hypoxemia and hypercapnia

Intractable hypoxemia is a characteristic feature of ARDS. Arterial blood gas analysis showed that PO_2 was significantly decreased in the ARDS group compared with the control group (Fig. 3A, $P < 0.05$). RSB

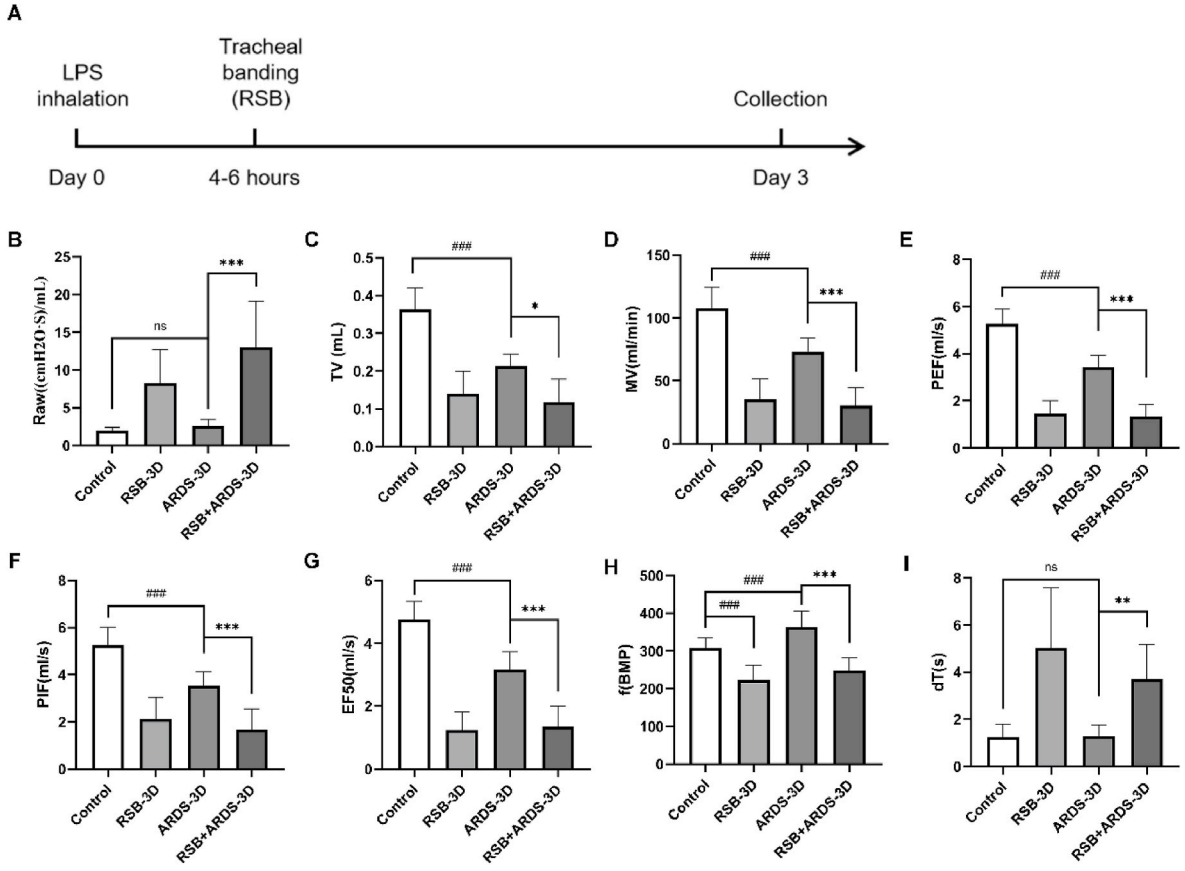

Fig. 2. Effect of RSB on the pulmonary function of mice with ARDS. (**A**) Timeline of animal experimental protocol. Changes in (**B**) Raw, (**C**) TV, (**D**) minute volume (MV), (**E**) peak expiratory flow (PEF), (**F**) peak inspiratory flow (PIF), (**G**) expiratory flow at the 50 % point of TV (EF50), (**H**) f, and (**I**) delta time (dT) measured by non-invasive double-chamber plethysmography (DCP). The values are indicated as mean ± SD (n = 8~10). $^{###}P < 0.001$, compared with the control group; $^{*}P < 0.05$, $^{**}P < 0.01$, $^{***}P < 0.001$, compared with the ARDS group.

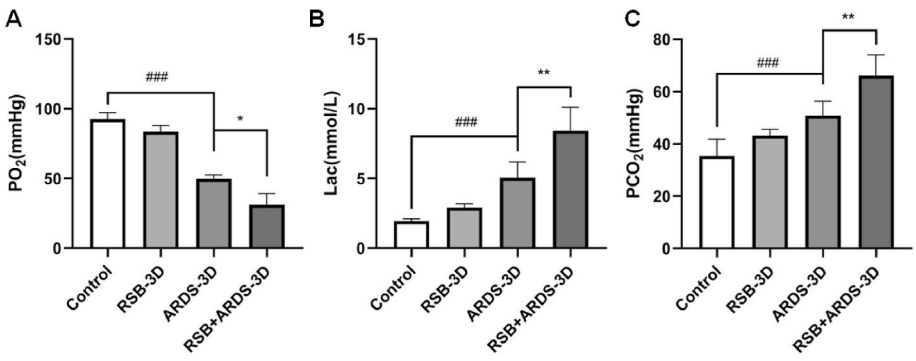

Fig. 3. Effect of RSB on arterial blood gas indices. Changes in (**A**) PO_2, (**B**) Lac, and (**C**) PCO_2 detected by a blood gas analyzer. The values are indicated as mean ± SD (n = 8~10). $^{###}P < 0.001$, compared with the control group; $^{*}P < 0.05$, $^{**}P < 0.01$, compared with the ARDS group.

treatment more effectively decreased PO_2 compared with ARDS alone (Fig. 3A, $P < 0.05$). The blood levels of lactic acid markedly increased in the ARDS and RSB + ARDS groups (Fig. 3B, $P < 0.05$). These results illuminated that RSB exacerbated ARDS-mediated hypoxemia. Moreover, PCO_2 significantly increased in the ARDS group compared with the control group (Fig. 3C, $P < 0.05$). PCO_2 was higher in the RSB + ARDS group compared with other groups (Fig. 3C, $P < 0.05$). Although there was no significant difference in base excess (Fig. s2A), it can be observed that the BE overall showed an increasing trend, displaying a similar change as PCO_2, indicating that RSB exacerbated hypercapnia. To summarize, RSB deteriorated LPS-induced hypoxemia and hypercapnia.

3.4. RSB accelerated LPS-induced pulmonary inflammation and damage

Pathological assessment of the lung is the "gold standard" to evaluate the severity of ARDS. The integrity of pulmonary alveoli and capillaries was maintained in the lung tissues of the control group with no enlargement or inflammatory infiltration. Segmental bronchial epithelial denudation with sloughed cells was observed after LPS. Moreover, distal alterations of alveolar ducts were noted, including hypercellular thickening of the alveolar septae, immune cell infiltration, and pneumocyte necrosis. Following RSB and LPS treatment, the capillaries and alveoli were congested, the number of neutrophils and extravasated monocytes was increased, and perivascular edema was observed. The results of H&E staining indicated that RSB promoted LPS-induced pulmonary pathological injury (Fig. 4A). The levels of IL-1β, IL-6, TNF-α, and total protein were significantly elevated in the BALF of the RSB + ARDS group compared with the ARDS group (Fig. 4B, $P < 0.05$), revealing that RSB significantly aggravated LPS-induced inflammation and cytokine release. In addition, FACS analysis was employed to measure the proportion of inflammatory cells in the lung and BALF. RSB markedly increased the proportion of $Ly6G^{+}CD11b^{+}$ neutrophils and decreased the proportion of $SiglecF^{+}CD11c^{+}$ alveolar macrophages in both BALF and lung ($P < 0.05$) (Fig. 4C–D). The number of inflammatory cells and cytokine levels were consistent with the severity of pathological damage. In summary, RSB significantly exacerbated LPS-induced pulmonary injury and inflammation.

3.5. Piezo1 was downregulated in ARDS with RSB

RSB induced mechanical stress on the lung by increasing airway pressure and reducing tidal volume. Mechanosensitive ion channels are the sensors and transducers of mechanical stimuli and confer mechanical stimuli into cellular response [20–22]. The expression levels of a large number of mechanosensitive ion channels were measured through qRT-PCR in this study. The mRNA expression level of Piezo1 was decreased in the ARDS group compared with the control group (Fig. 5A, $P < 0.05$). RSB further reduced Piezo1 expression compared with the ARDS group (Fig. 5A, $P < 0.05$). Immunohistochemical staining for Piezo1 also validated the results of q-PCR (Fig. 5G). The stains were dark in the parenchyma of the control group, decreased in the ARDS group, and was much lighter in the RSB + ARDS group ($P < 0.05$). Based on the above-mentioned results, it can be observed that the expression level of Piezo1 continuously declines with the aggravation of lung injury, consistent with the changes in the severity of the injury. The expression level of Trek1 did not show a significant difference between the experimental group and the control group (Fig. 5B). The expression levels of Aqp1, ENaC, and Cdh1 decreased in both the ARDS group and the RSB ARDS group ($P < 0.05$), but there was no significant difference between the two groups (Fig. 5C–E). Although the expression level of Cdh23 also decreased ($P < 0.05$) and there was a significant difference between the ARDS group and the RSB ARDS group ($P < 0.05$), its overall trend of change was not consistent with the severity of lung injury (Fig. 5F). Thus, we hypothesized that Piezo1 may be a key molecule involved in the exacerbation of LPS-induced lung injury by RSB.

4. Discussion

Mechanical stress-induced damage of the lung is involved in the pathogenesis of ARDS [23], especially VILI [24]. The role of mechanical stress has been widely recognized in ARDS, but it was limited to ventilator-induced mechanical forces. Since the concept of P-SILI was proposed in 2017 [3], the role of spontaneous breathing in ARDS has received much attention, but the exact mechanism has not been fully uncovered. The absence of a suitable animal model to investigate the mechanical consequences of spontaneous breathing in ARDS hindered the advancement of the field. Retamal and colleagues [25] showed that spontaneous breathing is associated with marked esophageal pressure swings, progressive hypoxemia, and lung injury compared with mechanical ventilation in the porcine model of lung collapse.

However, mechanical ventilation might improve esophageal pressure swings and alleviate lung damage. In this study, RSB was combined with LPS inhalation to measure the role of spontaneous respiratory mechanical forces in ARDS. RSB resulted in a significant airway resistance increase accompanied by tidal volume decrease in ARDS mice, suggesting that spontaneous respiratory restriction reduced ventilation. Besides, RSB aggravated carbon dioxide retention, indicating more severe type II respiratory failure. Importantly, the distinctive pulmonary pathological changes, more severe inflammatory cell infiltration, and increased IL-1β, IL-6, TNF-α, and total protein levels in BALF indicated that RSB exacerbated lung injury in mice with ARDS.

Tracheal banding increased airway resistance and decreased tidal volume, which resulted in a reactive increase in transmural pulmonary pressure swings, exacerbated mechanical stress of the lungs [4–7], and induced lung inflammation [4]. However, in this study, RSB did not induce obvious pulmonary inflammation or injury in normal animals. No significant inflammatory cell infiltration was observed in pathological assessment although there was a slight increase in inflammatory

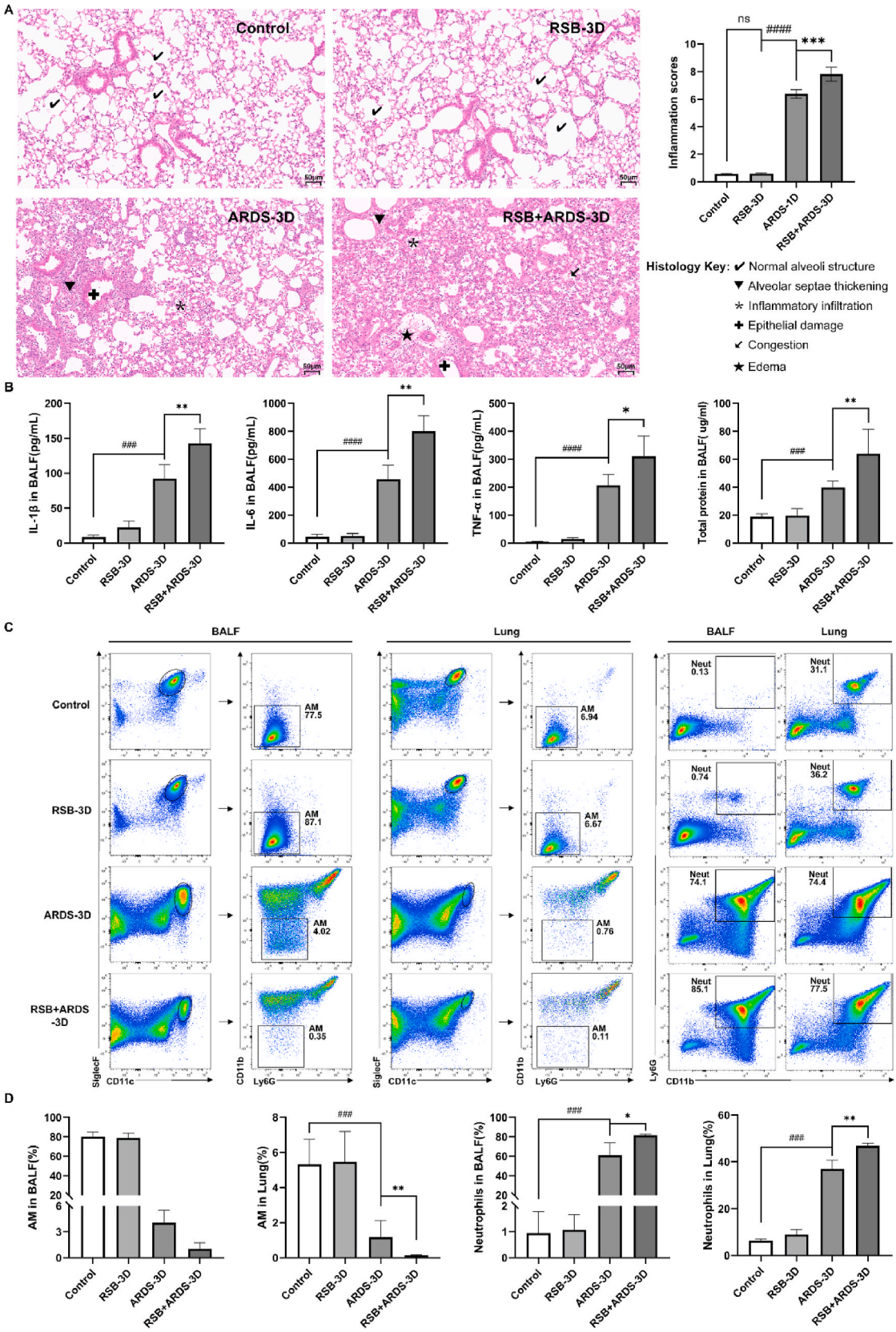

Fig. 4. Effect of RSB on the pulmonary inflammation of ARDS mice. (**A**) Pathological changes in pulmonary tissues were analyzed by hematoxylin and eosin staining (H&E, 200 × magnification). (**B**) Levels of IL-1β, IL-6, TNF-α, and total proteins in BALF were detected by ELISA and BCA. (**C**) The flow cytometry analysis of alveolar macrophages (AM) ($SiglecF^+CD11c^+CD11b^-$) and neutrophils (Neut) ($Ly6G^+CD11b^+$). (**D**)The proportion of alveolar macrophages and neutrophils in BALF and lung were analyzed by flow cytometry. The values are indicated as mean ± SD (n = 8~10). $^{###}P < 0.001$, $^{####}P < 0.0001$, compared with the control group; $^{*}P < 0.05$, $^{**}P < 0.01$, compared with the ARDS group.

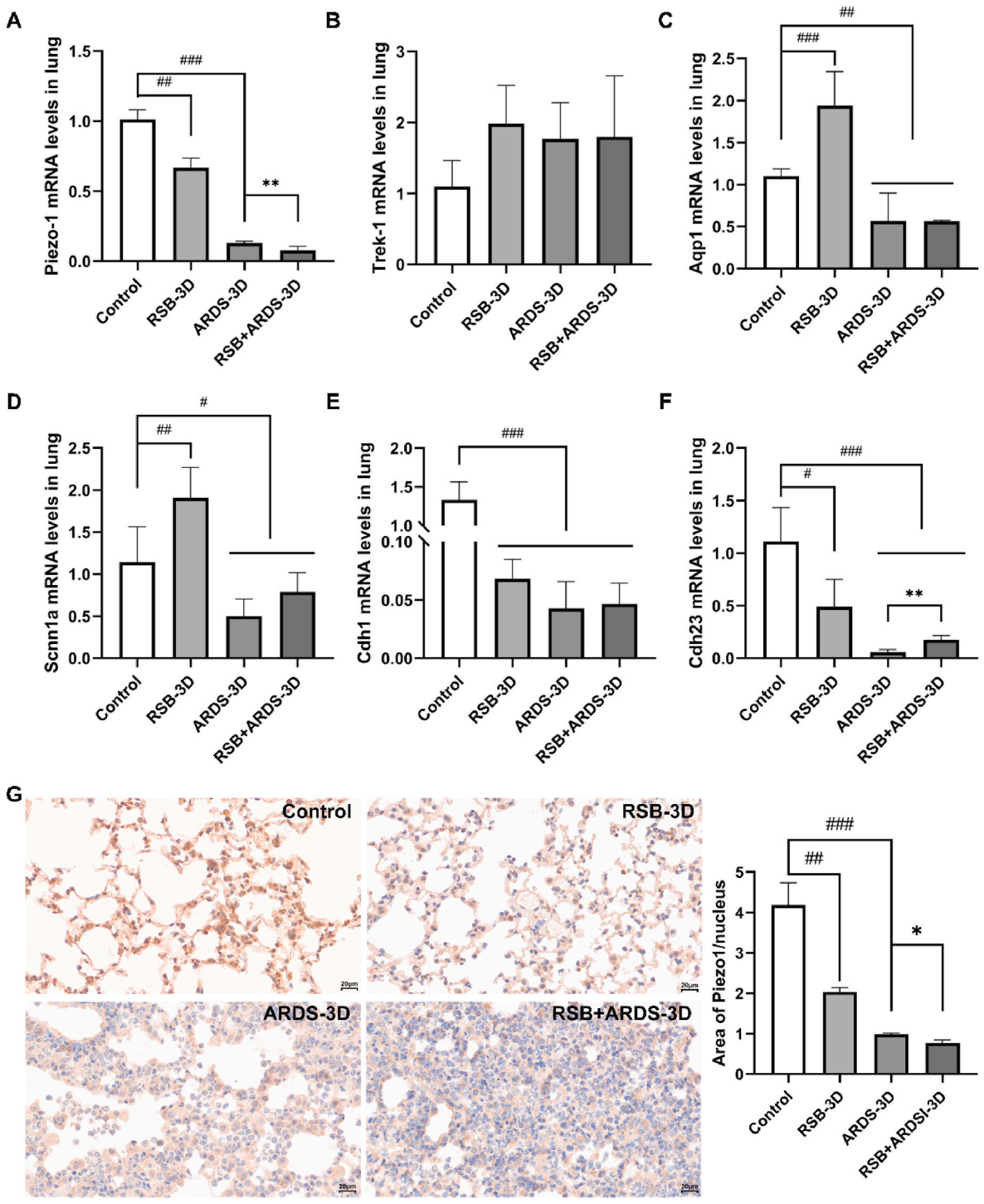

Fig. 5. Effect of RSB on the expression levels of mechanosensitive ion channels in lung tissues. The mRNA expression levels of (**A**) Piezo1, (**B**) Trek1, (**C**) Aqp1, (**D**) Scnn1α (ENaC), (**E**) Cdh1 and (**F**) Cdh23 were analyzed by quantitative real-time PCR. (**G**) The protein levels of Piezo1 in lung tissues were detected by immunohistochemistry (600x magnification). The values are indicated as mean ± SD (n = 8~10). $^{\#}P < 0.05$, $^{\#\#}P < 0.01$, $^{\#\#\#}P < 0.001$, compared with the control group; $^{**}P < 0.01$, compared with the ARDS group.

factor and total protein levels after 5 days. The differences in the results compared to published articles may be related to the different airway obstruction in the absence of respiratory monitoring during the modeling process. However, the RSB model only changed airway resistance and ventilation, indicating that this model is more suitable for exploring the role of spontaneous respiratory mechanical forces in ARDS.

In the acute phase of ARDS, resident alveolar macrophages release various proinflammatory mediators [26]. Meanwhile, neutrophils are the first immune cells recruited to the site of inflammation following stimulation by chemokines. They produce various proinflammatory cytokines, including IL-1β, IL-6 and TNF-α [27,28], damaging surrounding tissues and compromising gas exchange. High TNF-α expression has been previously reported in regions of high deformation induced by respiratory effort [29]. This was similar to the level of TNF-α in the BALF of RSB treatment for 5 days or RSB + ARDS for 3 days.

Besides, Toumpanakis and colleagues showed LPS inhalation did not affect respiratory system mechanics, but resistive breathing increased total resistance and augmenting lung inflammatory in combination with inhalational LPS exposure [8]. In this study, the combination of LPS and RSB not only aggravated lung pathological injury and inflammatory infiltration, but also deteriorated LPS-induced hypoxemia and hypercapnia. The results were concordant with characterization of P-SILI, being associated with markers of injury on the vascular side of the blood-gas barrier, such as hyperemia, edema, alveolar hemorrhage [30,31]. All results revealed that spontaneous respiratory mechanical force played an important role in the pathogenesis of ARDS.

Although the direct adverse effect of the increased mechanical forces cannot be excluded [32]. "Mechanosensitive" pathways play an important role in mechanical forces and mediate lung injury including resistive breathing and VILI [6,33–35]. MSCs could sense and transduce mechanical inputs into biochemical signals [9]. Therefore, MSCs were the focus on the effect of spontaneous respiration mechanical forces on lung injury. Here, Piezo1 (Piezo channel), ENaC (epithelial sodium channel), Aqp1 (associated with osmotic pressure and pH), Trek1 (two-pore domain potassium ion (K2P) channel), and Cdh23 (Mechano-electrical transduction channel) were measured. The mRNA expression levels of MSCs decreased significantly in ARDS induced by LPS inhalation except Trek1. Only Piezo1 were remarkably reduced in RSB + ARDS mice compared to ARDS, which was consistent with the severity of pulmonary damage. It has been reported that Piezo1 is involved in MV-mediated exacerbation of ARDS-associated pulmonary fibrosis [36]. The role of Piezo1 in spontaneous respiratory mechanical force-exacerbated ARDS need further validation.

There are also several limitations to our study. First, the RSB model was not assessed comprehensively, as only enhanced airway resistance and low tidal volume were identified in this study. Ventilatory parameters, such as pulmonary ventilation distribution and esophageal pressure swings, were not assessed because of small animal testing conditions. Second, only female mice were used to evaluate the effect of spontaneous respiratory mechanical force on ARDS. Although it has been reported there was no difference in the results between the genders in LPS-induced lung injury, male mice also need to be further studied to rule out hormonal regulation. Third, the expression level of Piezo1may be significantly negative in inflammatory marker levels and lung damage, that needs to be further studied by reverse validation.

5. Conclusion

RSB treatment deteriorated LPS-induced hypoxemia and exacerbated lung inflammation and damage in mice, and that was negative in expression level of Piezo1.

Ethics approval

The study protocol (IACUC-2023102) was approved by the Animal Care and Use Committee of Air Force Medical University (Xi'an, China) and was in accordance with the guidelines for the care and use of animals set by the Chinese government.

Funding

This work was supported by Natural Science Foundation of Shaanxi Province (2022JZ-58).

Availability of data and material

Not applicable.

CRediT authorship contribution statement

Zhigui Cai: Writing – review & editing, Writing – original draft, Visualization, Validation, Software, Formal analysis. **Huanhuan Zhang:** Writing – review & editing, Writing – original draft, Visualization, Validation, Software, Formal analysis. **Xingxing Guo:** Writing – original draft, Formal analysis. **Liqiang Song:** Funding acquisition.

Declaration of competing interest

All authors declared no potential conflicts of interest with respect to the research, author-ship, and/or publication of this article.

Acknowledgements

The authors would like to express their gratitude to EditSprings (https://www.editsprings.cn) for the expert linguistic services provided.

Appendix A. Supplementary data

Supplementary data to this article can be found online at https://doi.org/10.1016/j.bbrep.2024.101726.

References

[1] L.D.J. Bos, L.B. Ware, Acute respiratory distress syndrome: causes, pathophysiology, and phenotypes, Lancet 400 (10358) (Oct 1 2022) 1145–1156, https://doi.org/10.1016/s0140-6736(22)01485-4.
[2] G. Bellani, J.G. Laffey, T. Pham, et al., Epidemiology, patterns of care, and mortality for patients with acute respiratory distress syndrome in intensive care units in 50 countries, JAMA 315 (8) (Feb 23 2016) 788–800, https://doi.org/10.1001/jama.2016.0291.
[3] L. Brochard, A. Slutsky, A. Pesenti, Mechanical ventilation to minimize progression of lung injury in acute respiratory failure, Am. J. Respir. Crit. Care Med. 195 (4) (Feb 15 2017) 438–442, https://doi.org/10.1164/rccm.201605-1081CP.
[4] D. Toumpanakis, G.A. Kastis, P. Zacharatos, et al., Inspiratory resistive breathing induces acute lung injury, Am. J. Respir. Crit. Care Med. 182 (9) (Nov 1 2010) 1129–1136, https://doi.org/10.1164/rccm.201001-0116OC.
[5] C. Glynos, D. Toumpanakis, K. Loverdos, et al., Guanylyl cyclase activation reverses resistive breathing-induced lung injury and inflammation, Am. J. Respir. Cell Mol. Biol. 52 (6) (Jun 2015) 762–771, https://doi.org/10.1165/rcmb.2014-0092OC.
[6] D. Toumpanakis, A. Chatzianastasiou, V. Vassilakopoulou, et al., TRPV4 inhibition exerts protective effects against resistive breathing induced lung injury, Int. J. Chronic Obstr. Pulm. Dis. 17 (2022) 343–353, https://doi.org/10.2147/copd.S336108.
[7] D. Toumpanakis, E. Mizi, V. Vassilakopoulou, et al., Spontaneous breathing through increased airway resistance augments elastase-induced pulmonary emphysema, Int. J. Chronic Obstr. Pulm. Dis. 15 (2020) 1679–1688, https://doi.org/10.2147/copd.S256750.
[8] D. Toumpanakis, C. Glynos, P. Schoini, et al., Synergistic effects of resistive breathing on endotoxin-induced lung injury in mice, Int. J. Chronic Obstr. Pulm. Dis. 18 (2023) 2321–2333, https://doi.org/10.2147/copd.S424560.
[9] J.M. Kefauver, A.B. Ward, A. Patapoutian, Discoveries in structure and physiology of mechanically activated ion channels, Nature 587 (7835) (Nov 2020) 567–576, https://doi.org/10.1038/s41586-020-2933-1.
[10] Q. Jia, Y. Yang, X. Chen, S. Yao, Z. Hu, Emerging roles of mechanosensitive ion channels in acute lung injury/acute respiratory distress syndrome, Respir. Res. 23 (1) (Dec 20 2022) 366, https://doi.org/10.1186/s12931-022-02303-3.
[11] Y. Zhang, L. Jiang, T. Huang, et al., Mechanosensitive cation channel Piezo1 contributes to ventilator-induced lung injury by activating RhoA/ROCK1 in rats, Respir. Res. 22 (1) (Sep 21 2021) 250, https://doi.org/10.1186/s12931-021-01844-3.
[12] F. Khadangi, A.S. Forgues, S. Tremblay-Pitre, et al., Intranasal versus intratracheal exposure to lipopolysaccharides in a murine model of acute respiratory distress syndrome, Sci. Rep. 11 (1) (Apr 8 2021) 7777, https://doi.org/10.1038/s41598-021-87462-x.
[13] X. Zhang, X. Wei, Y. Deng, et al., Mesenchymal stromal cells alleviate acute respiratory distress syndrome through the cholinergic anti-inflammatory pathway, Signal Transduct. Targeted Ther. 7 (1) (Sep 5 2022) 307, https://doi.org/10.1038/s41392-022-01124-6.
[14] H.H. Yang, J.X. Duan, S.K. Liu, et al., A COX-2/sEH dual inhibitor PTUPB alleviates lipopolysaccharide-induced acute lung injury in mice by inhibiting NLRP3 inflammasome activation, Theranostics 10 (11) (2020) 4749–4761, https://doi.org/10.7150/thno.43108.
[15] S. Mailhot-Larouche, L. Deschênes, K. Lortie, et al., Assessment of respiratory function in conscious mice by double-chamber plethysmography, J. Vis. Exp. 137 (Jul 10 2018), https://doi.org/10.3791/57778.
[16] M. Xu, M.Q. Dong, F.L. Cao, et al., Tanshinone IIA reduces lethality and acute lung injury in LPS-treated mice by inhibition of PLA2 activity, Eur. J. Pharmacol. 607 (1–3) (Apr 1 2009) 194–200, https://doi.org/10.1016/j.ejphar.2009.02.003.

[17] M. Liu, Z. Shi, Y. Yin, et al., Particulate matter 2.5 triggers airway inflammation and bronchial hyperresponsiveness in mice by activating the SIRT2-p65 pathway, Front. Med. 15 (5) (Oct 2021) 750–766, https://doi.org/10.1007/s11684-021-0839-4.
[18] R. Yuan, M. Liu, Y. Cheng, et al., Biomimetic nanoparticle-mediated target delivery of hypoxia-responsive plasmid of angiotensin-converting enzyme 2 to reverse hypoxic pulmonary hypertension, ACS Nano 17 (9) (May 9 2023) 8204–8222, https://doi.org/10.1021/acsnano.2c12190.
[19] F. Khadangi, S. Tremblay-Pitre, A. Dufour-Mailhot, et al., Sensitive physiological readouts to evaluate countermeasures for lipopolysaccharide-induced lung alterations in mice, Am. J. Physiol. Lung Cell Mol. Physiol. 323 (1) (Jul 1 2022) L107–l120, https://doi.org/10.1152/ajplung.00073.2022.
[20] P. Delmas, T. Parpaite, B. Coste, PIEZO channels and newcomers in the mammalian mechanosensitive ion channel family, Neuron 110 (17) (Sep 7 2022) 2713–2727, https://doi.org/10.1016/j.neuron.2022.07.001.
[21] Y.L. Luo, J. Lacroix, Ion channels in biophysics and physiology: methods & challenges to study mechanosensitive ion channels, Adv. Exp. Med. Biol. 1349 (2021) 33–49, https://doi.org/10.1007/978-981-16-4254-8_3.
[22] L. Miles, J. Powell, C. Kozak, Y. Song, Mechanosensitive ion channels, axonal growth, and regeneration, Neuroscientist 29 (4) (Aug 2023) 421–444, https://doi.org/10.1177/10738584221088575.
[23] L. Gattinoni, T. Tonetti, M. Quintel, Regional physiology of ARDS, Crit. Care 21 (Suppl 3) (Dec 28 2017) 312, https://doi.org/10.1186/s13054-017-1905-9.
[24] Y. Xie, Y. Qian, Y. Wang, K. Liu, X. Li, Mechanical stretch and LPS affect the proliferation, extracellular matrix remodeling and viscoelasticity of lung fibroblasts, Exp. Ther. Med. 20 (5) (Nov 2020) 5, https://doi.org/10.3892/etm.2020.9133.
[25] M.C. Bachmann, P. Cruces, F. Díaz, et al., Spontaneous breathing promotes lung injury in an experimental model of alveolar collapse, Sci. Rep. 12 (1) (Jul 25 2022) 12648, https://doi.org/10.1038/s41598-022-16446-2.
[26] X. Huang, H. Xiu, S. Zhang, G. Zhang, The role of macrophages in the pathogenesis of ALI/ARDS, Mediat. Inflamm. (2018 2018) 1264913, https://doi.org/10.1155/2018/1264913.
[27] Y. Messaoud-Nacer, E. Culerier, S. Rose, et al., STING agonist diABZI induces PANoptosis and DNA mediated acute respiratory distress syndrome (ARDS), Cell Death Dis. 13 (3) (Mar 25 2022) 269, https://doi.org/10.1038/s41419-022-04664-5.
[28] C. Yang, C. Song, Y. Liu, et al., Re-Du-Ning injection ameliorates LPS-induced lung injury through inhibiting neutrophil extracellular traps formation, Phytomedicine 90 (Sep 2021) 153635, https://doi.org/10.1016/j.phymed.2021.153635.
[29] P. Cruces, J. Retamal, D.E. Hurtado, et al., A physiological approach to understand the role of respiratory effort in the progression of lung injury in SARS-CoV-2 infection, Crit. Care 24 (1) (Aug 10 2020) 494, https://doi.org/10.1186/s13054-020-03197-7.
[30] P. Cruces, B. Erranz, C. González, F. Diaz, Morphological differences between patient self-inflicted and ventilator-induced lung injury: an experimental study, Am. J. Respir. Crit. Care Med. 207 (6) (Mar 15 2023) 780–783, https://doi.org/10.1164/rccm.202207-1360LE.
[31] P. Cruces, B. Erranz, A. Pérez, et al., Non-invasive CPAP is a lung- and diaphragm-protective approach in self-inflicted lung injury, Am. J. Respir. Crit. Care Med. (Feb 6 2024), https://doi.org/10.1164/rccm.202309-1629LE.
[32] J.B. West, Invited review: pulmonary capillary stress failure, 1985, J. Appl. Physiol. 89 (6) (Dec 2000) 2483–2489, https://doi.org/10.1152/jappl.2000.89.6.2483. discussion 2497.
[33] D. Toumpanakis, V. Vassilakopoulou, I. Sigala, et al., The role of Src & ERK1/2 kinases in inspiratory resistive breathing induced acute lung injury and inflammation, Respir. Res. 18 (1) (Dec 13 2017) 209, https://doi.org/10.1186/s12931-017-0694-7.
[34] T. Vassilakopoulos, D. Toumpanakis, Can resistive breathing injure the lung? Implications for COPD exacerbations, Int. J. Chronic Obstr. Pulm. Dis. 11 (2016) 2377–2384, https://doi.org/10.2147/copd.S113877.
[35] G.F. Curley, J.G. Laffey, H. Zhang, A.S. Slutsky, Biotrauma and ventilator-induced lung injury: clinical implications, Chest 150 (5) (Nov 2016) 1109–1117, https://doi.org/10.1016/j.chest.2016.07.019.
[36] X.Z. Fang, M. Li, Y.X. Wang, et al., Mechanosensitive ion channel Piezo1 mediates mechanical ventilation-exacerbated ARDS-associated pulmonary fibrosis, J. Adv. Res. 53 (Nov) (2023) 175–186, https://doi.org/10.1016/j.jare.2022.12.006.